10 (2): 228-234 (2026)

Journal of Aviation

https://dergipark.org.tr/en/pub/jav

e-ISSN 2587-1676

Stochastical and Simultaneous Design of Mini Unmanned Helicopter Blade Taper and Its AFCS

Erdal Yeşilbaş[1]

[1]Erciyes University, Aeronautical Engineering Department, 38039, Melikgazi, Kayseri, Türkiye and Qatar Civil Aviation Authority (QCAA), Air Safety Department, Old Salata, Doha, Qatar (Erdal.Yesilbas@caa.gov.qa)

Article Info

Received: 27 March 2026
Revised: 01 May 2026
Accepted: 19 May 2026
Published Online: 30 May 2026

Keywords:
Mini unmanned helicopter
Redesign
Simultaneous and stochastical design
Automatic flight control system
Main rotor blade taper
SPSA

Corresponding Author: *Erdal Yeşilbaş*

RESEARCH ARTICLE

https://doi.org/10.30518/jav.1917228

Abstract

In this article, it is aimed to minimize cost of automatic flight control system (i.e., AFCS) for a mini unmanned helicopter (MUH) by simultaneously and stochastically redesigning main rotor blades' taper and PID gains of the AFCS. For minimization of autonomous flight cost index (AFCI) stochastical and simultaneous design approach is used over certain parameters (i.e., blade taper and gains of longitudinal and lateral PID controllers) while there are lower and upper constraints on these design parameters. A MUH is produced in Erciyes University Drone Laboratory (i.e., ERUDL) and called as Erciyes-Qtar-MUH. Its main rotor blades' taper ratio can change before flight. AFCS parameters and main rotor redesign parameter previously mentioned are stochastically and simultaneously designed for minimization of AFCI that captures rise time, settling time and overshoot of relevant trajectory trackings by using a certain stochastical optimization tool (i.e., simultaneous perturbation stochastical approximation: SPSA). Eventual results are used for making simulations of MUH. Via using simultaneous and stochastical redesign of passively morphing main rotor blade taper having MUH (i.e., Erciyes-Qtar-MUH) over previously mentioned redesign variables, a best MUH autonomous flight performance and a minimum AFCI are found. Simultaneous and stochastical redesign of passively morphing main rotor taper having MUH and its AFCS notion is honestly valuable for minimizing AFCS and maximizing autonomous flight performance any MUH. Composing an original notion for recovering AFCI of a MUH and contributing a new procedure performing simultaneous and stochastical redesign of a MUH having passively morphing main rotor taper and its AFCS strategy meanwhile existence of upper and lower constraints on design variables are main novelties of this research paper. Substantial progress for MUH AFCI save almost %38 with regard to the original MUH is found in this research paper.

1. Introduction

In the current century Unmanned Air Vehicles (i.e., UAVs) and also mini unmanned helicopters (i.e., MUHs) have been used in not only military operations but also marketable operations due to the much superiority with regard to the conventional manned aeronautical vehicles. Some of these features are inconsiderable operation costs, economical fabrication and readily varying composition. Initially, meanwhile civilian operations MUHs have been widely benefitted in airborne imagery, agri-food industry, and highway traffic management tasks. In addition, MUHs have been used in military operations, for instance, radar system jamming, destruction, and aerial reconnaissance in air force; for strategic and operational reconnaissance and surveillance and intervene on the battlefield in army; and for shadowing enemy fleets in navy (please visit references Austin, 2010; Valavanis, 2007; Bento, 2008 for many different MUH operations). The MUH used and produced for this article is in the class of mini UAV since it satisfies the criteria of maximum 2 hour endurance, maximum 10 km data link, and maximum 300 m flight altitude (see Bento, 2008 for details of the UAV classifications).

Meanwhile conventional UAV or MUH system design methodology, dynamical model of the aeronautical system that will be automatically flight controlled is given a priori to the aeronautical vehicle automatic flight control system (i.e., AFCS) engineer who has not any responsibility during conceptual or detailed design stages of this aeronautical system. However, it is public condition that the dynamical system and automatic flight control system design procedures are highly relevant (for this fact references Grigoriadis et. al., 1993; Grigoriadis et. al, 1996; Grigoriadis and Skelton, 1996; Oktay and Sultan, 2013 can be examined). Inconsiderable alterations in certain dynamical system parameters may enhance MUH autonomous flight performance substantially. The classical conventional design strategy may not contribute the best global final design fallouts in general. The better strategy is that the aeronautical vehicle which will be automatically controlled and the AFCS are critical to be simultaneously designed meanwhile minimizing an AFCI. In this research article this situation is evaluated and a MUH that

is Erciyes University Drone Laboratory (i.e., ERUDL) and called as Erciyes-Qtar-MUH and a HFCS are simultaneously designed via using helicopter main rotor blade design parameter (i.e., blade taper) and additionally MUH AFCS parameters (i.e., gains of longitudinal and lateral PID controllers) while minimizing AFCI capturing some autonomous flight trajectory tracking terms (i.e., rise time, settling time, and overshoot during longitudinal and lateral trajectory trackings) and while there are lower and upper constraints on these previously mentioned design parameters.

Significant developments and advancements for helicopter automatic flight control systems (i.e., AFCSs) for decreasing autonomous flight cost index (i.e, AFCI) have been occurred by benefitting simultaneous redesign methodologies over preceding years. Some of these mentioned redesign methodologies on helicopters are use of moving horizontal tailplane surface (please visit references Sherry, 1953; Stuart, 1961; Oktay and Sal, 2015 for different applications), reevaluating the helicopter blade qualities, for instance, flapping spring stiffness, chord length and taper before beginning the flight (that is named as passive morphing in the relevant expertise and benefitted in also this research article) or continuously changing different helicopter blade qualities, for example, radius and twist meanwhile the flight called (that is named as active morphing in the relevant expertise and not benefitted in this research article). As an example, in Oktay and Sultan, 2013 it was obtained that passive morphing was substantially valuable in order to reduce the AFCI of particular helicopter. The passively morphing properties in this relevant paper were radius, twist, linear mass density, flapping spring stiffness, chord, and angular speed of the blade. In another research in Oktay and Sal, 2017 blade taper which is also primary focus in this research article is considered for redesign of helicopter main rotor. The effect of simultaneous change in both blade root chord and taper on the AFCI of AFCS for a helicopter is researched. For helicopter AFCS variance-constrained controllers, specific output variance-constrained controllers are benefited. It was found from this paper that considerable decrease on AFCI can be obtained by choosing suitable AFCS controller gains and taper ratios. Additionally, in reference Vu et. al., 2013 the blade taper was researched for optimizing the hover performance. The design properties were the taper ratio, start of the taper on blade radius, and chord length on blade root. Some additional parameters such as the blade twist and coefficients of the airfoil distribution function were also considered in the relevant paper. After application of optimization, it was obtained that there is 7.4% reduction on the required horsepower and there is 6.5% increase on the figure of merit during hover. Furthermore, in Ozdemir and Kaya, 2006 flapwise bending vibration examination of a rotating, tapered cantilever Bernoulli–Euler beam similar with helicopter blade was investigated by benefitting the differential transform method (i.e., DTM). The impact of blade taper on also natural frequencies was also researched. It was obtained from the relevant study that the natural frequencies of a rotating, tapered cantilever Bernoulli–Euler beam can be detected with great accuracy via applying the DTM. References Ozdemir and Kaya, 2007; Kambampati and Ganguli, 2016; Oktay and Sultan, 2014; Ganguli, 2002; Sahasrabudhe et. al., 2007; Sal, 2020; Oktay, 2012; Sal, 2023; Oktay and Sal, 2016; Achaudhary and Bhushan, 2023 can be also visited for applications of different redesign – simultaneous design methodologies on helicopters and MUHs.

In this research article, initially, dynamical modeling of the any MUH system and effect of blade taper on these systems are considered in detail. After that, benefitted AFCS for our MUH flight control is shortly summarized. Then, applied optimization notion for stochastical and simultaneous design of our MUH blade taper and its AFCS is also given. Lastly, implementation results of stochastical and simultaneous redesign methodology are shared. In the MUH literature, this article is the first article which stochastically and simultaneously redesigns main rotor blade taper and its AFCS. In additional, for this intention a stochastical optimization methodology named as SPSA (i.e., simultaneous perturbation stochastic approximation) is also first time applied meanwhile existence of lower and upper constraints on the redesign parameters. These two contributions are the main novelties of this article. These approaches guarantee reaching the optimal outcomes confident and agile. It can be detected from the relevant literature that there is no similar research in the similar field. This investigation fulfills a stochastical and simultaneous redesign approach on MUHs for minimization of AFCI. Additionally, it is critical to note that this methodology requires a certain dynamical model for implementation.

2. Implemented Helicopter Models and Blade Redesign Parameters

In this section dynamical modelling of MUH which is named as Erciyes-Qtar-MUH and produced in ERUDL is presented. The essential steps of the MUH modeling are given below (please visit nomenclature at the Appendix for explanations of the symbols used here):

2.1. MUH Body Dynamical and Kinematical Equations:

Newton-Euler Equations (1) and (2), respectively are used in order to find the nondimensionalized MUH force (F1,F2,F3) and moment (M1,M2,M3) equations. The nondimensionalized kinematical Euler equations (K1,K2,K3) are also shared in Equation (3):

$$F1:\frac{d}{d\psi}\hat{u}+\hat{q}\,\hat{w}-\hat{r}\,\hat{v}+\frac{1}{\Omega^2 R}g\sin(\theta_A)=\frac{1}{\Omega^2 R}\frac{X}{m_{MUH}}\,\&$$
$$F2:\frac{d}{d\psi}\hat{v}+\hat{r}\,\hat{u}-\hat{p}\,\hat{w}-\frac{1}{\Omega^2 R}g\cos(\theta_A)\sin(\phi_A)=\frac{1}{\Omega^2 R}\frac{Y}{m_{MUH}}\,\& \quad (1)$$
$$F3:\frac{d}{d\psi}\hat{w}+\hat{p}\,\hat{v}-\hat{q}\,\hat{u}-\frac{1}{\Omega^2 R}g\cos(\theta_A)\cos(\phi_A)=\frac{1}{\Omega^2 R}\frac{Z}{m_{MUH}}$$

$$M1:\frac{d}{d\psi}\hat{p}-\hat{q}\,\hat{r}\left(\frac{I_{yy}}{I_{xx}}-\frac{I_{zz}}{I_{xx}}\right)-\frac{I_{xz}}{I_{xx}}\left(\hat{p}\,\hat{q}+\frac{d}{d\psi}\hat{r}\right)=\frac{1}{I_{xx}\,\Omega^2}L\,\&$$
$$M2:\frac{d}{d\psi}\hat{q}-\hat{p}\,\hat{r}\left(\frac{I_{zz}}{I_{yy}}-\frac{I_{xx}}{I_{yy}}\right)+\frac{I_{xz}}{I_{yy}}\left(\hat{p}^2-\hat{q}^2\right)=\frac{1}{I_{yy}\,\Omega^2}M\,\& \quad (2)$$
$$M3:\frac{d}{d\psi}\hat{r}-\hat{p}\,\hat{q}\left(\frac{I_{xx}}{I_{zz}}-\frac{I_{yy}}{I_{zz}}\right)-\frac{I_{xz}}{I_{zz}}\left(\hat{q}\,\hat{r}-\frac{d}{d\psi}\hat{p}\right)=\frac{1}{I_{zz}\,\Omega^2}N$$

$$K1:\hat{p}=\frac{d}{d\psi}\phi_A-\frac{d}{d\psi}\psi_A\sin(\theta_A)\,\&$$
$$K2:\hat{q}=\frac{d}{d\psi}\psi_A\cos(\theta_A)\sin(\phi_A)+\frac{d}{d\psi}\theta_A\cos(\phi_A)\,\& \quad (3)$$
$$K3:\hat{r}=\frac{d}{d\psi}\psi_A\cos(\theta_A)\cos(\phi_A)-\frac{d}{d\psi}\theta_A\sin(\phi_A)$$

2.2. MUH Dynamical and Aerodynamical Force and Moment Equations for any Blade

For a blade strip the infinitesimal aerodynamical force and moment equations in flapping frame (i.e., F), respectively are:

$$F: d_F\vec{F}_{aero} = \frac{I_b}{2R^3}\gamma \begin{bmatrix} 0 \\ -\left(\theta\, U_T^2 - U_P\, U_T\right)\frac{U_P}{U_T} - \frac{1}{a_0}\left(\delta_0 + \delta_2\left(\theta - \frac{U_P}{U_T}\right)^2\right) \\ \theta\, U_T^2 - U_P\, U_T \end{bmatrix} dx \quad \& \quad (4)$$

$$M: d_F\vec{M}_{aero} = \begin{bmatrix} 0 & -xR\,(d_F\vec{F}_{aero})_{III} & xR\,(d_F\vec{F}_{aero})_{II} \end{bmatrix}^T$$

Integrating these infinitesimal vectors along with the radius, the total aerodynamical force and moment for a whole blade can be found (visit also references Oktay, 2012; Leishman, 2006; Padfield, 2007).

2.3. MUH Multi-Blades/Main Rotor Dynamical and Aerodynamic Equations

The flapping motion of the any of all three main rotor blades can be shown via disregarding higher harmonic terms:

$$\beta_i(\psi) = \beta_0 + \beta_{1c}\cos(\psi_i) + \beta_{1s}\sin(\psi_i) \quad (5)$$

Above the azimuth angle of the ith blade is $\psi_i = \psi - (2\pi/3)(i-1),\ i = 1,...,3$ and $\beta_0, \beta_{1c}, \beta_{1s}$, are collective, longitudinal and lateral pieces, respectively.

2.4. MUH Blade Taper

In this research article blade taper is considered and implemented as structural redesign parameter. Therefore, it is included in formerly mentioned MUH dynamical and aerodynamical models. In Figure 1 MUH blade taper parameters are given, respectively. The blade taper affects both of blade root chord and blade tip chord. The magnitudes of impact on these previously mentioned roots are equal but in opposite ways. The blade root and tip chords can be expressed as a function of taper parameter as below:

$$c_{root_i} = (1+\xi_i)c_b \quad \text{and} \quad c_{tip_i} = (1-\xi_i)c_b \quad (6)$$

$$\Lambda_i = \frac{(1-\xi_i)c_b}{(1+\xi_i)c_b} = \frac{(1-\xi_i)}{(1+\xi_i)} \quad (7)$$

where Λ is the taper ratio and ξ is the taper parameter above. For the main rotor blade where the taper is not applied, $\Lambda = 0$, $\xi = 0$, and $c_{root} = c_{tip} = c_b$.

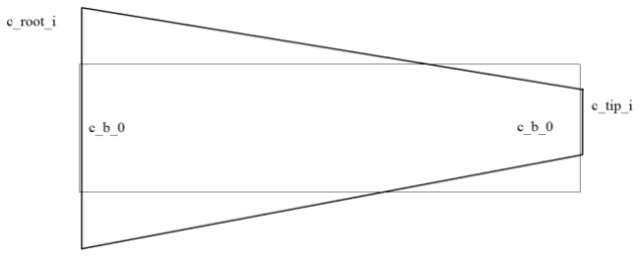


Figure 1. Application of taper on MUH blade

2.5. Assembly of Components Tapered Blades Having MUH

For creating dynamical models of our MUH all of previously mentioned considerations are assembled into the nonlinear equations of the MUH dynamical models. They can be defined in the generic implicit form:

$$f(\dot{x}, x, u) = 0 \quad (8)$$

where $f \in \mathbb{R}^{18}$, $x \in \mathbb{R}^{15}$ is the nonlinear state vector including the 9 fuselage states (i.e. 3 linear velocity states, 3 angular velocity states, 3 Euler angle states) and blade states (i.e. 3 flapping states) , and $u \in \mathbb{R}^4$ is the nonlinear control vector capturing 2 cyclic (i.e., longitudinal and lateral) controls and 1 collective control for the MUH main rotor and 1 collective control for MUH tail rotor. Meanwhile stochastical and simultaneous redesign notion of MUH and its AFCS, the formerly expressed MUH nonlinear models are linearized around different forward flight trim situations.

2.6. General Properties of our Erciyes-Qtar-MUH

In Figure 2 below flight test photos of our MUH called as Erciyes-Qtar-MUH and having passively morphing main rotor blade taper property is presented. Additionally, in Table 1 some of main properties of our MUH are given. In the first column of this table property, symbol and dimension of it are given, respectively. In the second column of this table physical value of the relevant parameter is shared.



Figure 2. Photos of Erciyes-Qtar-MUH

Table 1. Main Properties of our MUH

MUH Property, Symbol, Dimension	Physical Value of Relevant Property
Main rotor blade radius, R, [m]	0.7 m
Main rotor blade chord length, c_b, [m]	0.042 m
Main rotor angular speed, Ω, [rad/s]	150 rad/s
Main rotor blade twist, θ_{tw}	-0.12 rad
MUH engine system	Battery powered powerplant system
MUH total mass, m_{MUH}, [kg]	3.5 kg
MUH moment of inertia for pitching, I_{xx}, [$kg*m^2$]	$3.0029*10^{-3}$ $kg*m^2$
MUH moment of inertia for yawing, I_{yy}, [$kg*m^2$]	$3.0637*10^{-3}$ $kg*m^2$
MUH moment of inertia for rolling, I_{zz}, [$kg*m^2$]	$7.2935*10^{-4}$ $kg*m^2$
MUH product moment of inertia, I_{xz}, [$kg*m^2$]	$1.0381*10^{-4}$ $kg*m^2$
MUH main rotor blade lift curve slope, a_0, [1/rad]	5.73 / rad
MUH main rotor blade lock number, γ, [ ]	8.71
MUH number of blades for the main rotor, n_i, [ ]	3
NUH blade flapping spring stiffness, k_β, [N/rad]	21.2367
MUH main rotor hinge offset, e, [ ]	0.2
MUH main rotor blade inertia, I_b, [$kg*m^2$]	$8.1427*10^{-3}$ $kg*m^2$
MUH main rotor blade profile drag, δ_0, [ ]	0.01
MUH main rotor blade induced drag, δ_2, [ ]	0.4
MUH fuselage length, l_f, [m]	45 cm
MUH fuselage diameter, d_f, [m]	12 cm
MUH tail rotor thrust coefficient, c_T, [ ]	3.2935

3. Implemented AFCS for the Autonomous Flight

In this article for AFCS of our MUH it is selected a PID oriented hierarchical flight control system meanwhile relevant trajectory tracking. Basic features of this control system are shared next: Hierarchical flight control systems which are implemented inside of our MUH's AFC have three segments. These segments are external segment, middle segment and internal segment, respectively. Behaviors of MUH'S roll angle and pitch angle are stabilized within the internal segment via benefitting control signals received from main rotor longitudinal cyclic for longitudinal guidance and main rotor lateral pitch angle for lateral guidance. Following these, heading and altitude are stabilized within the middle segment of the flight control system. Eventually, tracking of x- and y-positions of MUH is made within the external segment. These types of flight control systems have 6 PID controllers within the AFCS block diagram. Via benefitting this block diagram, three reference trajectories (i.e., MUH altitude, MUH speed and MUH heading angle) can be tracked in most general form (visit Cai et. al., 2021; Dharmayanda et. al., 2010; Basri, 2017 for details and blocks).

4. Implemented Optimization Procedure

The stochastically and simultaneous bounded redesign of MUH main rotor blades' taper and PID gains of the AFCS for minimizing AFCI is given next:

$$\min_{k_{P_{lon}},k_{I_{lon}},k_{D_{lon}},\Lambda} J, \quad \text{where}$$

$$5 \le k_{P_{lon}} \le 95,\quad 0.5 \le k_{I_{lon}} \le 9.5,\quad 5 \le k_{D_{lon}} \le 95,\quad 0.75 \le \Lambda \le 1.25,$$

$$J = T_{r_{lon}} + T_{st_{lon}} + M_{p_{lon}} \tag{9}$$

The AFCI consists of rise time, settling time and overshoot during longitudinal trajectory tracking of MUH while there are lower and upper bounds on redesign parameters. There is a well-known information that guess of AFCI derivatives with regard to relevant design parameters seems analytically impossible. Therefore, a strong stochastic optimization methodology is crucial. For solving this redesign problem, SPSA approach is selected in this article. A short description of SPSA is shared next: Ψ demonstrates the vector of redesign variables (i.e., $k_{P_{lon}}, k_{I_{lon}}, k_{D_{lon}}, \Lambda$) here. During the standard SPSA, if $\Psi_{[k]}$ is the guess of Ψ at k-th iteration, then $\Psi_{[k+1]} = \Psi_{[k]} - \Psi_k g_{[k]}$. In this place, a_k and d_k are gain sequences, $g_{[k]}$ is the guess of the gradient of AFCI at $\Psi_{[k]}$, $g_{[k]} = \left[\frac{\Gamma_+ - \Gamma_-}{2d_k\Delta_{[k]1}} \ldots\ldots \frac{\Gamma_+ - \Gamma_-}{2d_k\Delta_{[k]p}}\right]^T$, $\Delta_{[k]} \in R^p$ is a vector of p mutually independent mean-zero random variables $\{\Delta_{[k]1} \ldots\ldots \Delta_{[k]p}\}$ fulfilling confident conditions (please visit

references Oktay and Sal, 2017; Song et. al., 2008; Sadegh and Spall, 1998; He et. al., 2003), Γ_+ and Γ_- are guesses of the AFCI computed at $\Psi_{[k]}+d_k\Delta_{[k]}$ and $\Psi_{[k]}-d_k\Delta_{[k]}$, respectively. As well, d, a, λ, Θ, S are extra SPSA parameters.

5. Effect of Stochastical and Simultaneous Design of MUH on AFCI

In this article meanwhile minimizing AFCI of a MUH via implementing stochastical and simultaneous redesign of main rotor blades' taper and PID gains of the AFCS during existence of lower and upper constraints on redesign parameters, SPSA methodology is selected. During this redesign problem, the longitudinal trajectory for our MUH controlled by AFCS is 5 degrees of helicopter pitch angle. After implementation of stochastical and simultaneous redesign notion rather than implementing traditional sequential notion, considerably more AFCI save is obtained. In Figure 3 below total AFCI, relative AFCI save, changes of longitudinal PID controller gains, and change of blade taper are shared, respectively. The relative AFCI save with regard to the initial preliminary situation (i.e., $k_{P_{lon}}=50, k_{I_{lon}}=5, k_{D_{lon}}=50, \Lambda=1.1$) is around %38 after implementing stochastical and simultaneous redesign notion. Additionally, the ultimate values of design parameters after implementation of stochastical and simultaneous redesign notion are $k_{P_{lon}}=85.2, k_{I_{lon}}=6.3, k_{D_{lon}}=46.2, \Lambda=0.751$.

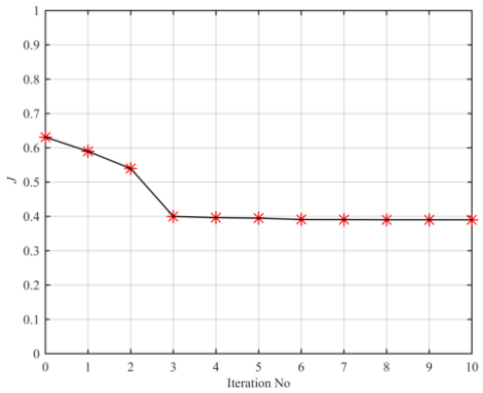


Figure 3. AFCI minimization of our MUH

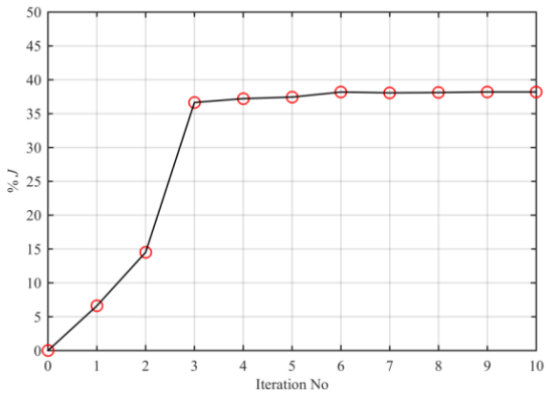


Figure 4. Relative AFCI save of our MUH

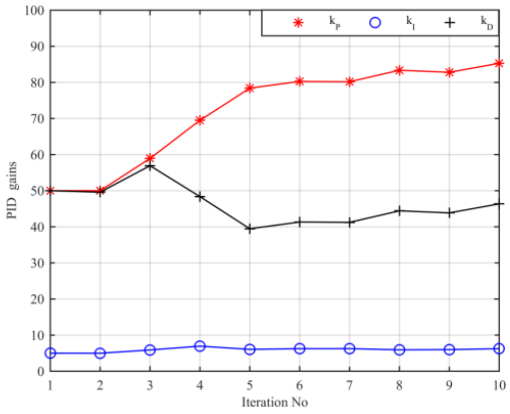


Figure 5. Changes of longitudinal PID controller gains

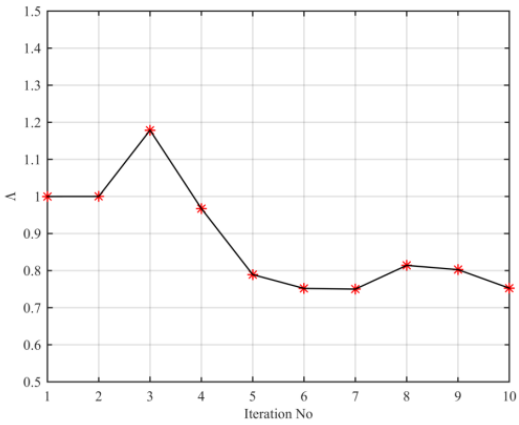


Figure 6. Change of blade taper

6. Effect of Stochastical and Simultaneous Design of MUH on CLRs

In this chapter effect of stochastical and simultaneous design of MUH on closed loop responses (i.e., CLRs) are also considered. Via benefitting Matlab/Simulink simulation environment achievement of our AFCS while existence of a minor turbulence within the MUH dynamical model is also investigated. The key MUH closed loop responses (i.e., CLRs) for longitudinal flight during existence of minor turbulence are given in Figure 7. In Figure 7 the x- axis demonstrates time in seconds and y- axis demonstrates input and outputs in degrees, respectively. It can be clearly extracted from Figure 7 that meanwhile existence of minor turbulence in the MUH dynamical system; our AFCS can robustly track the reference trajectory for MUH longitudinal flight. Furthermore, it can be detected from Figure 7 that parts of the AFCI (i.e., the settling time, rise time and overshoot values) are properly unimportant because of the reality that stochastical and simultaneous redesign notion is implemented in this research article. Besides, the additional states (e.g., u, q, and ϕ_A) which are not in critical interest for longitudinal trajectory tracking of AFCS are exposed to rapid and huge oscillations. Lastly, during existence of bound on control surface which is $\pm 20^0$ for longitudinal cyclic pitch angle, the desired longitudinal trajectory is autonomously tracked accomplishedly.

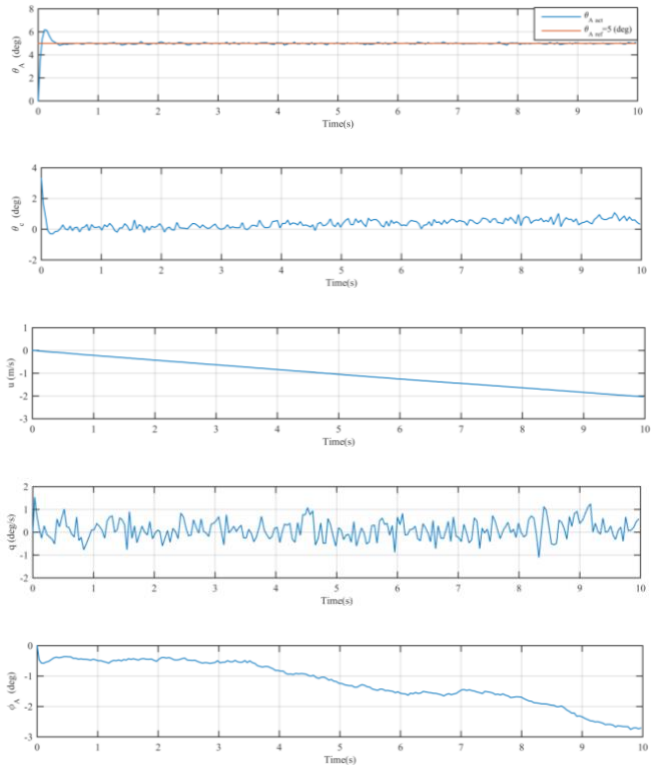


Figure 7. Main responses of Erciyes-Qtar-MUH

7. Conclusions

Stochastical and simultaneous redesign of mini unmanned helicopter (i.e., MUH) and its automatic flight control system (i.e., AFCS) over main rotor blades' taper and PID gains of the AFCS is considered for minimization of autonomous flight cost index (i.e., AFCI) of a specific MUH named as Erciyes-Qtar-MUH. A MUH was manufactured in Erciyes University Drone Laboratory (i.e., ERUDL). Its main rotor blades' taper ratio is allowed to be varied in a prescribed interval before flight. AFCS variables (i.e., gains of the PID controllers) and blade taper parameter are stochastically and simultaneously redesigned for minimization of AFCI that includes rise time, settling time and overshoot during reference trajectory tracking via implementing a certain stochastic optimization tool (i.e., simultaneous perturbation stochastic approximation: SPSA). These notions guaranteed reaching the optimal outcomes confident and agile. Outcomes found after implementation of stochastical and simultaneous redesign was benefitted for longitudinal flight simulations. Substantial progress for MUH AFCI save was found. It is almost %38 with regard to the initial not redesigned MUH. This result caused considerably less overshoot, less settling time and less rise time meanwhile autonomous tracking of longitudinal flight trajectory. Additionally, this consequence contributed positive effect on fuel consumption, carbon emission, and clean nature. Closed-loop responses (i.e., CLRs) during existence of minor turbulence for MUH were also researched and attractive outcomes (i.e., substantially low rise time, settling time and also overshoot) were reached. In the close future, it is planned to also consider varying blade taper throughout the flight duration for MUH main rotor in order to better minimize AFCI.

APPENDIX

Nomenclature:

Physical Parameter	Description
$\beta_0, \beta_c, \beta_s$	MUH collective, and longitudinal and lateral cyclics flapping states
$\beta_0 / s, \beta_c / s, \beta_s / s$ /s	MUH collective, and longitudinal and lateral cyclics flapping velocity states
u, v, w	MUH linear velocity states
p, q, r	MUH Angular velocity states
ϕ_A, θ_A, ψ_A	MUH attitude states
θ_c	MUH main rotor longitudinal cyclic control
U_P and U_T	MUH Perpendicular and tangential components of air velocity acting on the blade leading edge
γ	MUH main rotor blade lock number
a_0	MUH main rotor blade lift curve slope
δ_0 and δ_2	Parasite and induced drag coefficients
θ	MUH main rotor blade pitch angle
x	The nondimensional location of a generic point on the blade of MUH main rotor blade
Ω	The main rotor's angular speed of MUH
R	The main rotor radius of MUH
I_b	The main rotor blades inertia of MUH
M_a	The mass of the MUH
ψ	The blade's azimuth angle of MUH main rotor
Λ	MUH main rotor blade taper ratio
ξ	MUH main rotor blade taper parameter
$\wedge$	Any nondimensionalized quantity for MUH modeling

Abbreviation	Description
AFCS	Automatic Flight Control System
AFCI	Autonomous Flight Cost Index
CLR	Closed Loop Response
CLS	Closed Loop System
ERUDL	Erciyes University Drone Laboratory

Conflicts of Interest

The author declares that there is no conflict of interest regarding the publication of this paper.

Acknowledgement

No funding was received for conducting this study.

References

Achaudhary, A. and Bhushan, B. (2023). An improved teaching learning based optimization method to enrich the flight control of a helicopter system. Sadhana Journal, 48(222).

Austin, R. (2010). Unmanned aircraft systems. Wiley.

Basri, M. A. M. (2017). Trajectory tracking control of autonomous quadrotor helicopter using robust neural adaptive backstepping

approach. Journal of Aerospace Engineering, 31(2).
Bento, M. F. (2008). Unmanned Aerial Vehicles: An overview. Working papers, InsideGNSS, www.insidegnss.com
Cai, G., Chen, B. M. and Lee, T. H. (2011). Unmanned rotorcraft systems. Advances in Industrial Control, Springer.
Dharmayanda, H. R., Budiyono, A. and Kang, T. (2010). State-space identification and implementation of H∞ control design for small-scale helicopter. Aircraft Engineering and Aerospace Technology, 82(6): 340-352.
Ganguli, R. (2002) Optimum design of a helicopter rotor for low vibration using aeroelastic analysis and response surface methods. Journal of Sound and Vibration, 258(2): 327–344.
Grigoriadis, K. M., Carpenter, M. J., Zhu, G., and Skelton, R. E. (1993). Optimal redesign of linear systems. Proceedings of the American Control Conference, San Francisco, CA.
Grigoriadis, K. M., Zhu, G., and Skelton, R. E. (1996). Optimal Redesign of Linear Systems. Journal of Dynamic Systems, Measurement and Control, 118 (3), 598–605.
Grigoriadis, K. and Skelton, R. E. (1996). Minimum-energy covariance controllers. Automatica, 3(4), 569-578.
He, Y., Fu, M. C., Marcus, S. I. (2003). Convergence of simultaneous perturbation stochastic approximation for non-differentiable optimization. IEEE Transactions on Aerospace and Electronic Systems, 48(8):1459-1463.
Kambampati, S. and Ganguli, R. (2016). Nonrotating beams isospectral to tapered rotating beams. AIAA Journal, 54(2): 750–757.
Leishman, J. G. (2006). Principles of helicopter aerodynamics. Cambridge University Press.
Oktay, T. and Sultan, C. (2013). Simultaneous helicopter and control system design. Journal of Aircraft, 50(3), 206-222.
Oktay, T. and Sal, F. (2015). Helicopter control energy reduction using moving horizontal tail. The Scientific World Journal: Aerospace Engineering.
Oktay, T. and Sal, F. (2017). Effect of the simultaneous variation in blade root chord length and blade taper on helicopter flight control effort. International Journal of Aerospace Engineering.
Oktay, T. and Sultan, C. (2014). Flight control energy saving via helicopter rotor active morphing. AIAA Journal of Aircraft, 51(6): 1784-1805.
Oktay, T. (2012). Constrained control of complex helicopter models. Virginia Tech, PhD Dissertation, https://vtechworks.lib.vt.edu/items/e10a0b02-32f4-4dc9-8587-a85839e5ef7b.
Oktay, T. and Sal, F. (2016). Combined passive and active helicopter main rotor morphing for helicopter energy save. Journal of the Brazilian Society of Mechanical Sciences and Engineering, 38: 1511-1525.
Özdemir, Ö. and Kaya, M. O. (2006). Flapwise bending vibration analysis of a rotating tapered cantilever Bernoulli–Euler beam by differential transform method. Journal of Sound and Vibration, 289(1-2): 413–420.
Özdemir, Ö. and Kaya, M. O. (2007). Energy expressions and free vibration analysis of a rotating double tapered Timoshenko beam featuring bending–torsion coupling. International Journal of Engineering Science, 45(2–8), 562–586.
Padfield, G. D. (2007). Helicopter flight dynamics. AIAA Education Series.
Sadegh, P. and Spall, J. C. (1998). Optimal random perturbations for multivariable stochastic approximation using a simultaneous perturbation gradient approximation. IEEE Transactions on Automatic Control, 43(10):1480-1484.
Sahasrabudhe, V., Tischler, M., Cheng, R., Stumm, A., and Lavin, M. (2007). Balancing CH-53K handling qualities and stability margin requirements in the presence of heavy external loads. Proceedings of the American Helicopter Society 63rd Forum, Virginia Beach, VA, USA.
Sal, F. (2020). Effects of the actively morphing root chord and taper on helicopter energy. Aircraft Engineering and Aerospace Technology, 92(2):264-270.
Sal, F. (2023). Simultaneous swept anhedral helicopter blade tip shape and control-system design. Aircraft Engineering and Aerospace Technology, 95(1): 101-112.
Sherry, J. (1953). Helicopter stabilizer. U.S. Patent 2,630,985, March 10.
Song, Q., Spall, J. C., and Soh, Y. C. (2008). Robust neural network tracking controller using simultaneous perturbation stochastic approximation. IEEE Transactions on Neural Networks, 19(5):817-835.
Stuart, J. (1961). Horizontal tail plane for helicopters. U.S. Patent 2,979,286.
Valavanis, K. (2007). Advances in unmanned aerial vehicles: State of the art and the road to autonomy, ser. Microprocessor-based and intelligent systems engineering. Springer-Verlag, Berlin.
Vu, N. A., Lee, J. W., and Shu, J. I. (2013). Aerodynamic design optimization of helicopter rotor blades including airfoil shape for hover performance. Chinese Journal of Aeronautics, 26(1): 1–8.

Cite this article: Yesilbas, E. (2026). Stochastical and Simultaneous Design of Mini Unmanned Helicopter Blade Taper and Its AFCS. Journal of Aviation, 10(2), 228-234.

This is an open access article distributed under the terms of the Creative Commons Attribution 4.0 International License

Copyright © 2026 Journal of Aviation https://javsci.com - https://dergipark.org.tr/en/pub/jav